Electronic Supplementary Information (ESI)

K, Rb-Hydroxyborates Series with Deep-Ultraviolet $KRbB_5O_8(OH)$ Possessing Moderate Second Harmonic Generation Response

Aihaimaitijiang Ababaikeri,[a] Xueting Pan,[a] Xueling Hou[a,b] and Jian Han[a,b,*]

[a]*Research Center for Crystal Materials; State Key Laboratory of Functional Materials and Devices for Special Environmental Conditions; Xinjiang Key Laboratory of Functional Crystal Materials; Xinjiang Technical Institute of Physics and Chemistry, Chinese Academy of Sciences, 40-1 South Beijing Road, Urumqi 830011, China*

[b]*Center of Materials Science and Optoelectronics Engineering, University of Chinese Academy of Sciences, Beijing 100049, China*

[*]*To whom correspondence should be addressed, E-mail: hanjian@ms.xjb.ac.cn*

EXPERIMENTAL SECTION

1. Single Crystal and Polycrystalline Powder Synthesis

Single crystals of compound **I** were grown via a high-temperature solution method in a closed system, using $Li_2B_4O_7$ and H_3BO_3 as flux. Analytically pure reagents (purity ＞ 99 %, Aladdin Chemical Industry Co., Ltd.) $Li_2B_4O_7$ (0.147 g, 1 mmol), H_3BO_3 (0.150 g, 2.5 mmol), RbF (0.270 g, 2.5 mmol), KF (0.080 g, 1.4 mmol) were weighed in the molar ratio of 1:2.5:2.5:1.4 and transferred into a tidy silica glass tube (Φ10 mm × 100 mm) and was flame-sealed under 10^{-3} Pa, the tube was put in the programmable muffle furnace (Temperature control accuracy ± 1 °C), then elevated to 480 °C in 24 h and annealed at this temperature for 12 h, slowly cooled to 325 °C, then 250 °C in 62 h, further to room temperature in 5 h. For polycrystalline powder samples of **I**, KOH (0.244 g), Rb_2CO_3 (0.370 g), and H_3BO_3 (0.935 g) were used to synthesize via hydrothermal method according to stoichiometric ratios. The mixtures were ground thoroughly in an agate mortar and sealed with a Teflon liner (23 mL) in an autoclave, heated in the oven (Temperature control accuracy ± 0.1 °C) at 220 °C for 4 days, and then cooled slowly to room temperature at 1.5 °C/h. The chemical reaction of **I** is as follows:

$$K_2CO_3 + Rb_2CO_3 + 10H_3BO_3 = 2KRbB_5O_8(OH) + 14H_2O + 2CO_2\uparrow$$

K_2CO_3 (0.247 g, 0.345 g), Rb_2CO_3 (0.451 g, 0.347 g), and H_3BO_3 (0.927 g, 0.933 g) were used to synthesize single crystals of **II** and **III** via hydrothermal method under mild condition according to stoichiometric ratios (0.5:0.5:6 and 0.8:0.5:5, respectively). The mixtures were ground thoroughly in an agate mortar and sealed with a Teflon liner (23 mL) in an autoclave, heated in the oven at 220 °C for 4 days, and cooled slowly to room temperature at 1.2 °C/h. The chemical reaction of **II** is as follows:

$$K_2CO_3 + Rb_2CO_3 + 12H_3BO_3 = 2KRbB_6O_9(OH)_2 + 16H_2O + 2CO_2\uparrow$$

The purity of compound **I** was inspected by a Bruker D2 PHASER powder X-ray diffractometer (Cu-Kα radiation with λ = 1.5418 Å, 2θ = 10-70 °, *d* = 0.02 °, and counting time = 1s/step, accuracy equal to or better than ± 0.02 ° 2 θ). A comparison of powder X-ray data in terms of experimental and calculated patterns is given in a typical Rietveld-style difference plot. A full Rietveld refinement was carried out by using the GSAS II software.[1] As shown in Figure S2, the observed and calculated XRD patterns, and the difference profile are in purple, green, and blue, respectively. The olive vertical lines indicate the Bragg reflection position of **I**. The fitted profile matches well with the experimental data derived from the single crystal crystallographic information file (CIF), giving the reasonable *R* values of R_P = 0.0414 and R_{wP} = 0.0684 with all of the observed Bragg reflections indexed into the space group of $Pca2_1$, indicating the phase purity of the sample.

As is emphasized in the title “with Moderate Second Harmonic Generation Response”, **I**, with a non-centrosymmetric space group, is fully characterized as a representative and centrosymmetric **II** and **III** are partially characterized, for we failed to obtain the highly purified powder samples of them.

2. Single Crystal X-ray Diffraction

Single crystals of the compounds were selected for structure determination with the help of an optical polarizing microscope. Structure data were collected by D8 Venture X-ray diffractometer using monochromatic Mo-Kα radiation (λ = 0.71073 Å, angle deviation = 0.005 °) at 296 K, and integrated with the SAINT program.[2] Data absorption corrections were completed with the SCALE program for the area detector. All calculations were implemented with the SHELXTL crystallographic software package.[3] Atomic position refinements were implemented with full-matrix least-squares techniques, and final least-squares refinement on F_o^2 with data having $F_o^2 \geq 2\sigma(F_o^2)$. The heavy atom method was applied to determine the atoms (fluorine can be easily identified from hydroxyl, and hydrogen atoms can be positioned based on the comprehensive consideration of the reasonability of the hydrogen bonds, Q peak, electron cloud density map, and the surrounding environment of the related atoms, which will also give a better indicator of the data), and symmetry element correctness was verified with the PLATON program.[4] The crystal information and final structure refinement data are listed in Table S1, and the atomic position coordinate parameters, selected bond lengths, and angles are offered in Tables S2, S3, and S4.

3. Infrared Spectrum

To specify the nature of the covalent bonding and atomic groups in the structure of **I**, the IR performances were measured by Shimadzu IR Affinity-1 Fourier transform infrared spectrometer at room temperature in the 400-4000 cm^{-1} range with a resolution of 2 cm^{-1}. The samples were mixed thoroughly with dried KBr at the ratio of sample: KBr = 1: 100.

4. UV–vis-IR Diffuse Reflectance Spectrum

Shimadzu SolidSpec-3700 DUV spectrophotometer (a resolution of 0.1 nm) was used in an atmosphere of flowing nitrogen to determine the absorption edge of **I**. The optical diffuse reflectance spectrum was collected in the wavelength range of 190-2600 nm at room temperature.

5. Energy Dispersive Spectroscopy

Elemental analyses of **I**, **II**, and **III** were conducted on the surface of a clean single crystal by using a field emission scanning electron microscope (SEM, SUPRA55 VP, a resolution of 1 nm), which was equipped with an energy-dispersive X-ray spectroscope (EDS, BRUKER X-flash-sdd-5010).

6. Thermal Analysis

Thermal gravimetry (TG) and differential scanning calorimetry (DSC) were carried out on a simultaneous NETZSCH STA 449 F3 thermal analyzer instrument (accuracy equal to 1 %) under a flowing N_2 atmosphere to examine the thermal stability of **I**, **II**, and **III** (small amounts of single crystals were selected from the single crystal samples of

II and **III** for TG and DSC test, 20 mg). The samples were placed in the Pt crucible and heated from 40 to 600 °C at a rate of 5 °C·min^{-1}.

7. SHG Intensity Measurement

The Kurtz-Perry method[5] was used to measure the second harmonic generation (SHG) signals of polycrystalline. Since the SHG efficiency is closely related to the particle size, polycrystalline specimens were ground and sieved into a series of distinct size ranges: 38-54, 54-87, 87-105, 105-150, 150-200, and 200-250 μm. The specimens were pressed between cover slides and taped to a 1 mm thick aluminum or plastic holder with an 8 mm diameter groove. KDP crystals were also ground and sifted into the same grain size range for comparison with known SHG materials. Then the specimens were laid in an opaque case and subjected to pulsed laser light. The Q-switched Nd: YAG laser was adopted for visible SHG measurement at 1064 nm. The back flash on the specimens was limited by a cut-off filter, and the second harmonic was detected through an interference filter (530 ± 10 nm). The photomultiplier tube was connected to the RIGOL DS1052E 50 MHz oscilloscope. Then the process was repeated with the standard KDP to calculate the ratio of the output intensity of SHG. Index-matching fluid was not used in all experiments.

8. Birefringence Assessment

The birefringence of **I**, **II**, and **III** was experimentally assessed under the cross-polarizing microscope (ZEISS Axio Scope. 5, magnification factor 40-1000 times) equipped with a Berek compensator, and the average wavelength of the light source is 546.1 nm. The boundary lines of the first-, second-, and third-order interference color could be observed clearly, and the relative error was relatively small. For the sake of improving the precision of the experiment, the crystal of **I**, **II**, and **III** with high optical quality was selected using the polarizing microscope. The method of how birefringence is measured can be expressed as the following formula (1):

$$R = |Ng-Np| \times T = \Delta n \times T \quad (1)$$

Here, R, Ng, Np, T, and Δn represent the optical path difference, the refractive index of fast light, the refractive index of slow light, the thickness of the crystal, and the experimental difference of refractive index, respectively.[6]

9. Theoretical Calculations

The CASTEP program,[7] a plane-wave pseudo-potential code based on the Density Functional Theory (DFT), has been used to further elucidate the band structure and optoelectric properties of compound **I**. During the calculations, the generalized gradient approximation (GGA) with Perdew-Burke-Ernzerhof (PBE) function[8] was adopted. The norm-conserving pseudo-potential (NCP)[9,10] with the kinetic energy Cut-off 830 eV was applied, and the Monkhorst-Pack K-point mesh was set as 6 x 7 x 4 in the Brillouin zone. During the calculation of electronic properties, the convergent conditions and other parameters used in the calculation were kept fixed as in the auto-setting of the CASTEP code. To get closer to the experimental band gap results, we used the nonlocal exchange hybrid functional Heyd−Scuseria−Ernzerhof (HSE06). The

scissors operators are set as the difference between GGA and HSE06 gaps to achieve quantitative agreement with the experiment, in which interband optical property was calculated using ab initio self-consistent energy bands, wave functions, and an empirical energy-dependent self-energy correction.[11]

Table S1a. Crystallographic and structural refinement data for $KRbB_5O_8(OH)$.

Formula sum	$KRbB_5O_8(OH)$
Formula weight(g mol^{-1})	323.63
Crystal system	Orthorhombic
Space group	$Pca2_1$
a (Å)	8.5736(13)
b (Å)	7.5326(12)
c (Å)	13.072(2)
V (Å^3)	844.2(2)
Z	4
ρ_{cal} (g cm^{-3})	2.546
μ (mm^{-1})	6.385
F (000)	616.0
2θ (°)	5.408 to 50.752
Limiting indices	$-10 \le h \le 10$, $-8 \le k \le 9$, $-15 \le l \le 15$
Data/restraints/parameters	1505/8/148
Reflections collected / unique	5715 / 1505 [R(int) = 0.0776]
Completeness (%)	99.9
GOF (F^2)	1.052
Final R indices[$F_o^2 > 2\sigma(F_c^2)$][a]	R_1 = 0.0394, wR_2 = 0.0872
Final R indices (all data)[a]	R_1 = 0.0427, wR_2 = 0.0894
Largest diff. peak and hole (e·Å^{-3})	0.68 and -0.44

[a] $R_1 = \Sigma||F_o|-|F_c||/\Sigma|F_o|$ and $wR_2 = [\Sigma[w(F_o^2-F_c^2)^2]/\Sigma[w(F_o^2)^2]]^{1/2}$ for $F_o^2 > 2\sigma(F_c^2)$

Table S1b. Crystallographic and structural refinement data for $KRbB_6O_9(OH)_2$.

Formula sum	$KRbB_6O_9(OH)_2$
Formula weight(g mol^{-1})	367.45
Crystal system	Monoclinic
Space group	$P2_1/n$
a (Å)	9.1030(5)
b (Å)	6.6379(3)
c (Å)	16.3616(9)
β (deg.)	91.866(3)
V (Å^3)	988.12(9)
Z	4
ρ_{calcd} (g/cm^3)	2.470
μ (mm^{-1})	5.485
F (000)	704
2θ (°)	4.982 to 55.000
Limiting indices	$-11 \le h \le 11$, $-8 \le k \le 8$, $-20 \le l \le 21$
Data/restraints/parameters	2274/2/180
Reflections collected / unique	13478/ 2274 [R(int) = 0.0841]
Completeness (%)	100.0
GOF (F^2)	1.086
Final R indices[$F_o^2 > 2\sigma(F_c^2)$]^a	R_1 = 0.0548, wR_2 = 0.1347
Final R indices (all data)^a	R_1 = 0.0694, wR_2 = 0.1408
Largest diff. peak and hole (e·Å^{-3})	1.14 and -0.85

$^aR_1 = \Sigma ||F_o| - |F_c|| / \Sigma |F_o|$ and $wR_2 = [\Sigma [w(F_o^2-F_c^2)^2] / \Sigma [w(F_o^2)^2]]^{1/2}$ for $F_o^2 > 2\sigma(F_c^2)$

Table S1c. Crystallographic and structural refinement data for $K_{3.3}Rb_{0.7}B_{10}O_{15}(OH)_4$.

Formula sum	$K_{3.3}Rb_{0.7}B_{10}O_{15}(OH)_4$
Formula weight(g mol^{-1})	604.76
Crystal system	Monoclinic
Space group	*C*2/*c*
a (Å)	18.144(4)
b (Å)	6.9056(14)
c (Å)	13.445(3)
β (°)	95.93(3)
V (Å^3)	1675.6(6)
Z	4
ρ_{cal} (g/cm^3)	2.397
μ (mm^{-1})	3.000
F (000)	1178
2θ (°)	4.514 to 54.986
Limiting indices	$-23 \le h \le 23$, $-8 \le k \le 8$, $-17 \le l \le 17$
Data/restraints/parameters	1918/0/152
Reflections collected / unique	13727 / 1918 [*R*(int) = 0.0525]
Completeness (%)	99.9
GOF (F^2)	1.130
Final *R* indices[$F_o^2 > 2\sigma(F_o^2)$][a]	R_1 = 0.0373, wR_2 = 0.1035
Final *R* indices (all data)[a]	R_1 = 0.0420, wR_2 = 0.1065
Largest diff. peak and hole (e·Å^{-3})	0.97and – 0.39

[a] $R_1 = \Sigma||F_o|-|F_c||/\Sigma|F_o|$ and $wR_2 = [\Sigma[w(F_o^2-F_c^2)^2]/\Sigma[w(F_o^2)^2]]^{1/2}$ for $F_o^2 > 2\sigma(F_c^2)$

Table S2a. Atomic coordinates ($\times 10^4$), equivalent isotropic displacement parameters ($Å^2 \times 10^3$), and BVS for $KRbB_5O_8(OH)$.

Atom	*Wyck*	S.O.F	*x/a*	*y/b*	*z/c*	$U_{eq}(Å^2)$	BVS
K_1|Rb_1	4a	0.5|0.5	1541(1)	10789(2)	5727(1)	30(1)	1.096
K_2|Rb_2	4a	0.5|0.5	3058(1)	3660(1)	3403(1)	21(1)	1.076
B(1)	4a	1	5786(10)	10004(12)	3250(7)	18(2)	3.057
B(2)	4a	1	3977(13)	4499(14)	6380(8)	21(2)	3.095
B(3)	4a	1	3570(11)	7525(12)	7028(8)	17(2)	3.027
B(4)	4a	1	3097(10)	6694(14)	5224(8)	19(2)	3.019
B(5)	4a	1	3211(10)	8356(11)	3480(9)	16(2)	3.063
O(1)	4a	1	2705(7)	6989(9)	4242(5)	23(1)	2.015
O(2)	4a	1	4856(7)	8749(8)	3654(4)	20(1)	1.990
O(3)	4a	1	7267(7)	10025(8)	3640(4)	22(1)	2.100
O(4)	4a	1	2045(7)	7624(8)	7470(4)	19(1)	1.976
O(5)	4a	1	5322(7)	11221(8)	2523(5)	18(1)	2.040
O(6)	4a	1	3476(6)	7969(8)	5921(4)	17(1)	2.221
O(7)	4a	1	4278(7)	5718(8)	7105(5)	23(1)	2.052
O(8)	4a	1	4460(8)	2774(9)	6436(6)	31(2)	1.218[p]
O(9)	4a	1	3142(7)	4908(9)	5518(5)	26(2)	2.041

U_{eq} is defined as one-third of the trace of the orthogonalized U_{ij} tensor, [p] protonated oxygen atom (the pair of electrons that form the O-H bond are both supplied by oxygen, so oxygen is equivalent to losing an electron).

Table S2b. Atomic coordinates ($\times 10^4$), equivalent isotropic displacement parameters ($Å^2 \times 10^3$), and BVS for $KRbB_6O_9(OH)_2$.

Atom	*Wyck*	S.O.F	*x/a*	*y/b*	*z/c*	$U_{eq}(Å^2)$	BVS
K_1|Rb_1	4e	0.5|0.5	10139(1)	11079(1)	3447(1)	24(1)	1.125
K_2|Rb_2	4e	0.5|0.5	9854(1)	3158(1)	8773(1)	20(1)	0.917
B(1)	4e	1	7256(7)	2976(11)	6570(4)	22(1)	3.091
B(2)	4e	1	7838(7)	5362(10)	5484(4)	21(1)	3.042
B(3)	4e	1	7625(7)	1837(10)	5153(4)	21(1)	3.072
B(4)	4e	1	7577(8)	8287(11)	4500(5)	24(1)	3.046
B(5)	4e	1	8182(8)	6203(12)	3314(5)	26(2)	3.056
B(6)	4e	1	5645(8)	6810(11)	3561(4)	24(1)	3.104
O(1)	4e	1	9180(5)	5238(8)	2852(3)	38(1)	2.055
O(2)	4e	1	8594(5)	7539(7)	3889(3)	26(1)	2.042
O(3)	4e	1	6724(5)	5776(7)	3133(3)	30(1)	2.032
O(4)	4e	1	4283(5)	6591(8)	3242(3)	36(1)	1.959
O(5)	4e	1	6025(5)	7918(7)	4234(3)	26(1)	1.883
O(6)	4e	1	7879(5)	7331(7)	5293(3)	26(1)	2.101
O(7)	4e	1	7708(6)	3850(7)	4904(3)	31(1)	2.122
O(8)	4e	1	7779(5)	466(7)	4557(3)	27(1)	1.077[p]
O(9)	4e	1	7374(5)	1392(6)	5944(3)	23(1)	1.925
O(10)	4e	1	7915(5)	4872(7)	6296(3)	26(1)	2.085
O(11)	4e	1	8054(5)	2420(8)	7316(3)	30(1)	1.250[p]

U_{eq} is defined as one-third of the trace of the orthogonalized U_{ij} tensor, [p] protonated oxygen atom.

Table S2c. Atomic coordinates ($\times 10^4$), equivalent isotropic displacement parameters ($Å^2 \times 10^3$), and BVS for $K_{3.3}Rb_{0.7}B_{10}O_{15}(OH)_4$.

Atom	*Wyck*	S.O.F	*x/a*	*y/b*	*z/c*	$U_{eq}(Å^2)$	BVS
K_1|Rb_1	8f	0.65|0.35	5631(1)	3591(1)	4340(1)	19(1)	1.164
K(2)	8f	1	2164(1)	6000(1)	3472(1)	20(1)	1.095
B(1)	8f	1	7237(2)	9059(6)	5991(3)	21(1)	3.057
B(2)	8f	1	5352(2)	8311(5)	3292(3)	17(1)	3.006
B(3)	8f	1	4179(2)	6496(5)	3092(3)	19(1)	3.009
B(4)	8f	1	3704(2)	3307(6)	3542(3)	21(1)	3.018
B(5)	8f	1	6082(2)	8847(5)	4962(3)	20(1)	3.023
O(1)	4e	1	5000	9508(4)	2500	18(1)	1.637
O(2)	8f	1	3644(1)	5416(3)	3501(2)	23(1)	2.033
O(3)	8f	1	7073(1)	7475(4)	6513(2)	23(1)	2.091
O(4)	8f	1	5724(1)	9495(3)	4094(2)	21(1)	2.202
O(5)	8f	1	4049(1)	7097(4)	2119(2)	23(1)	1.733
O(6)	8f	1	4806(1)	6977(3)	3677(2)	23(1)	2.074
O(7)	8f	1	5886(1)	7299(4)	5489(2)	24(1)	2.049
O(8)	8f	1	4073(1)	2652(4)	2701(2)	27(1)	1.161[p]
O(9)	8f	1	6721(1)	9907(4)	5294(2)	27(1)	2.124
O(10)	8f	1	7914(1)	9919(4)	6123(2)	31(1)	1.363[p]

U_{eq} is defined as one-third of the trace of the orthogonalized U_{ij} tensor, [p] protonated oxygen atom.

Table S3a. Selected bond lengths (Å) and angles (deg.) for $KRbB_5O_8(OH)$.

Bond	Length	Bond	Length
K_1|Rb_1-O(6)	2.708(6)	B(1)-O(2)	1.345(10)
K_1|Rb_1-O(6)#1	2.801(5)	B(1)-O(3)	1.369(12)
K_1|Rb_1-O(5)#2	2.858(6)	B(1)-O(5)	1.379(11)
K_1|Rb_1-O(3)#1	2.865(6)	B(2)-O(7)	1.345(12)
K_1|Rb_1-O(8)#3	3.059(7)	B(2)-O(8)	1.365(12)
K_1|Rb_1-O(2)#1	3.090(6)	B(2)-O(9)	1.370(12)
K_1|Rb_1-O(4)	3.326(6)	B(3)-O(4)	1.432(11)
K_1|Rb_1-O(8)#4	3.354(7)	B(3)-O(6)	1.487(11)
K_1|Rb_1-O(9)#3	3.404(7)	B(3)-O(5)#10	1.487(11)
K_2|Rb_2-O(1)	2.753(7)	B(3)-O(7)	1.493(10)
K_2|Rb_2-O(3)#4	2.874(6)	B(4)-O(1)	1.346(12)
K_2|Rb_2-O(7)#6	2.884(6)	B(4)-O(6)	1.363(12)
K_2|Rb_2-O(5)#7	2.910(6)	B(4)-O(9)	1.399(12)
K_2|Rb_2-O(9)	2.921(6)	B(5)-O(4)#8	1.447(13)
K_2|Rb_2-O(7)#8	3.049(6)	B(5)-O(2)	1.458(10)
K_2|Rb_2-O(4)#8	3.227(6)	B(5)-O(3)#1	1.479(10)
K_2|Rb_2-O(2)#4	3.307(6)	B(5)-O(1)	1.497(12)
K_2|Rb_2-O(8)#8	3.423(8)	O(4)-B(3)-O(5)#10	112.0(7)
O(2)-B(1)-O(3)	114.4(7)	O(4)-B(3)-O(7)	113.1(7)
O(3)-B(1)-O(5)	121.1(7)	O(1)-B(4)-O(9)	115.3(9)
O(2)-B(1)-O(5)	124.5(8)	O(6)-B(4)-O(9)	119.2(8)
O(8)-B(2)-O(9)	114.6(8)	O(1)-B(4)-O(6)	125.5(9)
O(7)-B(2)-O(9)	121.7(9)	O(4)#8-B(5)-O(1)	107.5(6)
O(7)-B(2)-O(8)	123.6(8)	O(3)#1-B(5)-O(1)	108.3(7)
O(5)#10-B(3)-O(7)	106.9(7)	O(2)-B(5)-O(1)	108.4(7)
O(6)-B(3)-O(7)	107.0(6)	O(2)-B(5)-O(3)#1	109.8(6)
O(5)#10-B(3)-O(6)	108.4(7)	O(4)#8-B(5)-O(3)#1	111.1(7)
O(4)-B(3)-O(6)	109.4(7)	O(4)#8-B(5)-O(2)	111.5(8)

Symmetry codes: #1 x-1/2,-y+2,z; #2 -x+1/2,y,z+1/2; #3 x,y+1,z; #4 x-1/2,-y+1,z; #5 x+1/2,-y+2,z; #6 -x+1,-y+1,z-1/2; #7 x,y-1,z; #8 -x+1/2,y,z-1/2; #9 x+1/2,-y+1,z; #10 -x+1,-y+2,z+1/2

Table S3b. Selected bond lengths (Å) and angles (deg.) for $KRbB_6O_9(OH)_2$.

Bond	Length	Bond	Length
K_1|Rb_1-O(2)	2.844(5)	B(1)-O(11)	1.448(8)
K_1|Rb_1-O(4)#1	2.850(5)	B(1)-O(10)	1.471(8)
K_1|Rb_1-O(8)#2	2.887(5)	B(1)-O(9)	1.474(8)
K_1|Rb_1-O(6)#3	2.895(4)	B(1)-O(4)#11	1.473(8)
K_1|Rb_1-O(9)#4	2.944(4)	B(2)-O(6)	1.345(8)
K_1|Rb_1-O(1)#2	3.045(6)	B(2)-O(10)	1.367(8)
K_1|Rb_1-O(3)#1	3.051(5)	B(2)-O(7)	1.384(8)
K_1|Rb_1-O(11)#4	3.129(5)	B(3)-O(8)	1.345(8)
K_1|Rb_1-O(10)#3	3.239(4)	B(3)-O(9)	1.354(8)
K_2|Rb_2-O(11)	2.892(4)	B(3)-O(7)	1.400(8)
K_2|Rb_2-O(5)#5	2.904(5)	B(4)-O(8)#2	1.461(8)
K_2|Rb_2-O(9)#6	3.000(4)	B(4)-O(6)	1.463(9)
K_2|Rb_2-O(6)#7	3.012(5)	B(4)-O(2)	1.469(9)
K_2|Rb_2-O(1)#4	3.022(6)	B(4)-O(5)	1.484(8)
K_2|Rb_2-O(8)#8	3.056(5)	B(5)-O(2)	1.338(8)
K_2|Rb_2-O(3)#8	3.306(5)	B(5)-O(1)	1.361(9)
K_2|Rb_2-O(4)#8	3.307(6)	B(5)-O(3)	1.381(8)
K_2|Rb_2-O(10)#7	3.333(5)	B(6)-O(4)	1.337(8)
K_2|Rb_2-O(5)#7	3.386(5)	B(6)-O(5)	1.360(8)
K_2|Rb_2-O(7)#8	3.410(5)	B(6)-O(3)	1.404(9)
O(11)-B(1)-O(10)	106.1(5)	O(8)#2-B(4)-O(5)	107.3(5)
O(4)#11-B(1)-O(10)	107.3(5)	O(8)#2-B(4)-O(2)	107.3(5)
O(11)-B(1)-O(4)#11	109.1(5)	O(6)-B(4)-O(5)	109.7(5)
O(9)-B(1)-O(10)	111.0(5)	O(6)-B(4)-O(2)	110.6(5)
O(11)-B(1)-O(9)	111.0(5)	O(8)#2-B(4)-O(6)	110.7(5)
O(4)#11-B(1)-O(9)	112.1(5)	O(2)-B(4)-O(5)	111.1(5)
O(6)-B(2)-O(10)	117.2(6)	O(1)-B(5)-O(3)	116.1(6)
O(10)-B(2)-O(7)	119.6(6)	O(2)-B(5)-O(1)	121.8(6)
O(6)-B(2)-O(7)	123.2(6)	O(2)-B(5)-O(3)	122.1(6)
O(8)-B(3)-O(7)	115.3(6)	O(4)-B(6)-O(3)	114.0(6)
O(9)-B(3)-O(7)	119.9(6)	O(5)-B(6)-O(3)	120.3(6)
O(8)-B(3)-O(9)	124.8(6)	O(4)-B(6)-O(5)	125.7(6)

Symmetry codes: #1 -x+3/2,y+1/2,-z+1/2; #2 x,y+1,z; #3 -x+2,-y+2,-z+1; #4 -x+2,-y+1,-z+1; #5 x+1/2,-y+3/2,z+1/2; #6 -x+3/2,y+1/2,-z+3/2; #7 -x+3/2,y-1/2,-z+3/2; #8 x+1/2,-y+1/2,z+1/2; #9 -x+2,-y+1,-z+2; #10 x+1/2,-y+3/2,z-1/2 #11 -x+1,-y+1,-z+1; #12 x,y-1,z; #13 x-1/2,-y+3/2,z+1/2

Table S3c. Selected bond lengths (Å) and angles (deg.) for $K_{3.3}Rb_{0.7}B_{10}O_{15}(OH)_4$.

Bond	Length	Bond	Length
$K_1\|Rb_1$-O(7)#1	2.852(2)	B(1)-O(3)	1.350(4)
$K_1\|Rb_1$-O(4)#2	2.855(2)	B(1)-O(10)	1.358(4)
$K_1\|Rb_1$-O(6)	2.868(3)	B(1)-O(9)	1.385(4)
$K_1\|Rb_1$-O(6)#1	2.886(2)	B(2)-O(1)#3	1.444(4)
$K_1\|Rb_1$-O(8)#3	2.922(3)	B(2)-O(4)	1.461(4)
$K_1\|Rb_1$-O(10)#4	2.958(3)	B(2)-O(6)	1.484(4)
$K_1\|Rb_1$-O(7)	3.001(3)	B(2)-O(5)#3	1.521(4)
$K_1\|Rb_1$-O(2)#1	3.137(3)	B(3)-O(6)	1.356(4)
$K_1\|Rb_1$-O(5)#3	3.206(3)	B(3)-O(5)	1.370(4)
$K_1\|Rb_1$-O(9)#2	3.391(3)	B(3)-O(2)	1.382(4)
K(2)-O(2)	2.712(3)	B(4)-O(8)	1.445(5)
K(2)-O(9)#5	2.760(3)	B(4)-O(2)	1.461(4)
K(2)-O(3)#1	2.770(3)	B(4)-O(7)#1	1.492(4)
K(2)-O(3)#6	2.826(3)	B(4)-O(3)#1	1.505(4)
K(2)-O(8)#7	2.845(3)	B(5)-O(7)	1.351(5)
K(2)-O(10)#8	2.876(3)	B(5)-O(4)	1.352(4)
K(2)-O(4)#5	3.009(3)	B(5)-O(9)	1.404(4)
O(10)-B(1)-O(9)	116.2(3)	O(6)-B(3)-O(5)	122.1(3)
O(3)-B(1)-O(9)	121.6(3)	O(2)-B(4)-O(3)#1	106.8(3)
O(3)-B(1)-O(10)	122.1(3)	O(8)-B(4)-O(2)	108.8(3)
O(4)-B(2)-O(5)#3	106.5(3)	O(7)#1-B(4)-O(3)#1	108.8(3)
O(6)-B(2)-O(5)#3	108.2(3)	O(2)-B(4)-O(7)#1	109.9(3)
O(1)-B(2)-O(5)#3	109.0(2)	O(8)-B(4)-O(3)#1	110.9(3)
O(1)-B(2)-O(6)	110.6(3)	O(8)-B(4)-O(7)#1	111.5(3)
O(1)-B(2)-O(4)	111.0(3)	O(4)-B(5)-O(9)	114.2(3)
O(4)-B(2)-O(6)	111.3(3)	O(7)-B(5)-O(9)	120.0(3)
O(6)-B(3)-O(2)	118.9(3)	O(7)-B(5)-O(4)	125.8(3)
O(5)-B(3)-O(2)	118.9(3)		

Symmetry codes: #1 -x+1,-y+1,-z+1; #2 x,y-1,z; #3 -x+1,y,-z+1/2; #4 -x+3/2,-y+3/2,-z+1; #5 x-1/2,y-1/2,z; #6 x-1/2,-y+3/2,z-1/2; #7 -x+1/2,y+1/2,-z+1/2; #8 -x+1,-y+2,-z+1

Table S4a. Anisotropic displacement parameters for $KRbB_5O_8(OH)$.

Atom	U_{11}	U_{22}	U_{33}	U_{23}	U_{13}	U_{12}
$K_1\|Rb_1$	28(1)	40(1)	22(1)	-3(1)	2(1)	15(1)
$K_2\|Rb_2$	28(1)	16(1)	19(1)	-4(1)	5(1)	1(1)
B(1)	17(4)	21(4)	14(5)	2(4)	4(4)	-1(3)
B(2)	26(5)	23(5)	15(5)	0(4)	-1(4)	-1(4)
B(3)	20(5)	17(5)	14(4)	-4(4)	0(4)	3(4)
B(4)	14(4)	22(5)	21(5)	5(4)	-1(4)	2(4)
B(5)	16(2)	16(2)	17(2)	0(1)	0(1)	-1(1)
O(1)	22(3)	30(4)	18(3)	2(3)	-3(3)	-8(3)
O(2)	17(3)	23(3)	18(4)	3(2)	-3(2)	0(2)
O(3)	17(3)	25(3)	23(4)	7(3)	-2(3)	-1(2)
O(4)	18(3)	25(3)	13(3)	-1(3)	3(2)	-2(2)
O(5)	16(3)	23(3)	14(3)	8(2)	1(2)	0(2)
O(6)	22(3)	19(3)	11(3)	-2(2)	1(2)	-3(2)
O(7)	32(4)	22(3)	14(3)	0(3)	-4(3)	6(3)
O(8)	39(4)	18(3)	34(4)	-1(3)	-17(3)	0(3)
O(9)	34(4)	22(3)	22(4)	-2(3)	-12(3)	0(3)

Table S4b. Anisotropic displacement parameters for $KRbB_6O_9(OH)_2$.

Atom	U_{11}	U_{22}	U_{33}	U_{23}	U_{13}	U_{12}
K_1|Rb_1	24(1)	26(1)	22(1)	4(1)	-2(1)	-3(1)
K_2|Rb_2	18(1)	15(1)	26(1)	-1(1)	-5(1)	-3(1)
B(1)	18(3)	23(4)	24(3)	-4(3)	-1(3)	-1(3)
B(2)	24(3)	17(3)	22(3)	-3(3)	-2(3)	-4(3)
B(3)	25(3)	14(3)	25(3)	-3(3)	-1(3)	-1(3)
B(4)	27(3)	17(3)	29(4)	-3(3)	-5(3)	0(3)
B(5)	23(3)	26(4)	28(4)	-6(3)	-3(3)	-1(3)
B(6)	28(3)	20(3)	23(3)	1(3)	-2(3)	1(3)
O(1)	24(2)	44(3)	46(3)	-19(3)	2(2)	-1(2)
O(2)	25(2)	23(2)	30(2)	-7(2)	0(2)	-3(2)
O(3)	24(2)	30(3)	36(3)	-13(2)	1(2)	1(2)
O(4)	22(2)	52(3)	36(3)	-18(2)	1(2)	-2(2)
O(5)	26(2)	22(2)	31(2)	-6(2)	0(2)	2(2)
O(6)	36(2)	19(2)	24(2)	-2(2)	-4(2)	-2(2)
O(7)	52(3)	20(2)	22(2)	0(2)	-5(2)	1(2)
O(8)	39(2)	20(2)	24(2)	-1(2)	0(2)	-2(2)
O(9)	27(2)	18(2)	25(2)	-2(2)	0(2)	-3(2)
O(10)	35(2)	21(2)	23(2)	-3(2)	-1(2)	-4(2)
O(11)	34(2)	31(3)	24(2)	5(2)	-8(2)	-4(2)

Table S4c. Anisotropic displacement parameters for $K_{3.3}Rb_{0.7}B_{10}O_{15}(OH)_4$.

Atom	U_{11}	U_{22}	U_{33}	U_{23}	U_{13}	U_{12}
K_1|Rb_1	19(1)	16(1)	22(1)	0(1)	6(1)	0(1)
K_2	16(1)	24(1)	21(1)	10(1)	6(1)	9(1)
B(1)	22(2)	20(2)	19(2)	0(1)	1(1)	-4(1)
B(2)	19(2)	17(2)	16(2)	-1(1)	-1(1)	0(1)
B(3)	18(2)	16(2)	22(2)	-1(1)	-1(1)	1(1)
B(4)	20(2)	20(2)	23(2)	3(1)	-1(1)	-4(1)
B(5)	20(2)	20(2)	21(2)	-2(1)	0(1)	-1(1)
O(1)	18(2)	16(2)	18(2)	0	-2(1)	0
O(2)	20(1)	21(1)	28(1)	2(1)	3(1)	-2(1)
O(3)	18(1)	25(1)	25(1)	6(1)	-3(1)	-4(1)
O(4)	25(1)	19(1)	19(1)	0(1)	-3(1)	-3(1)
O(5)	20(1)	26(1)	21(1)	3(1)	-2(1)	-7(1)
O(6)	23(1)	23(1)	22(1)	5(1)	-2(1)	-6(1)
O(7)	20(1)	26(1)	25(1)	5(1)	-5(1)	-6(1)
O(8)	28(1)	27(1)	27(1)	2(1)	6(1)	7(1)
O(9)	26(1)	27(1)	26(1)	7(1)	-6(1)	-7(1)
O(10)	24(1)	32(1)	35(2)	12(1)	-7(1)	-9(1)

Table S5. Peak assignments of $KRbB_5O_8(OH)$.

No	Absorption peaks (cm^{-1})	Mode description
1	1455	Uv(BO_3)
2	1361	Uas(BO_3)
3	840	U_S(BO_3)
4	1000	Uas(BO_4)
5	727	r(BO_4, BO_3)
6	3381, 3570	U(OH)

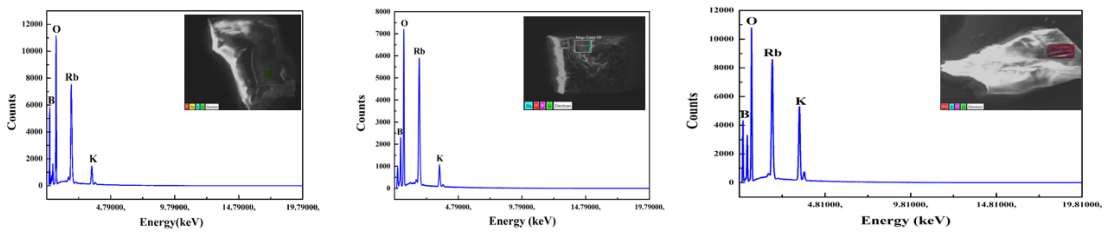

Figure S1. Energy-dispersive X-ray spectroscopic spectra of $KRbB_5O_8(OH)$, $KRbB_6O_9(OH)_2$, and $K_{3.3}Rb_{0.7}B_{10}O_{15}(OH)_4$.

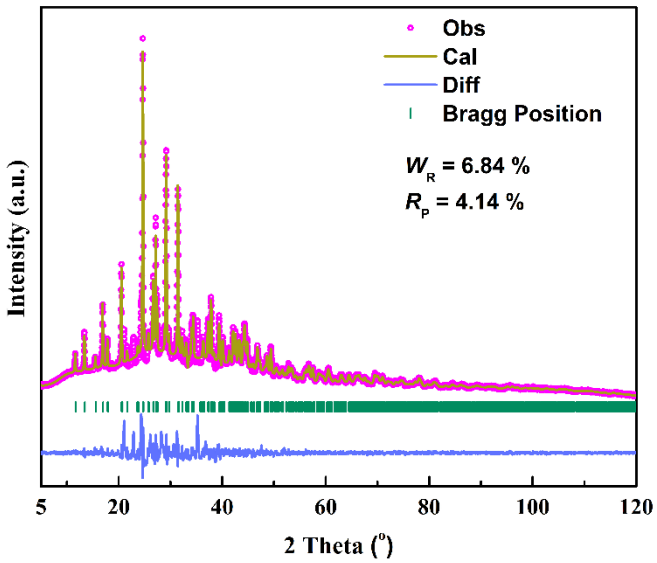

Figure S2. Rietveld refinement of the powder XRD profile of $KRbB_5O_8(OH)$ polycrystalline. A full Rietveld refinement was performed by using the GSAS II software.

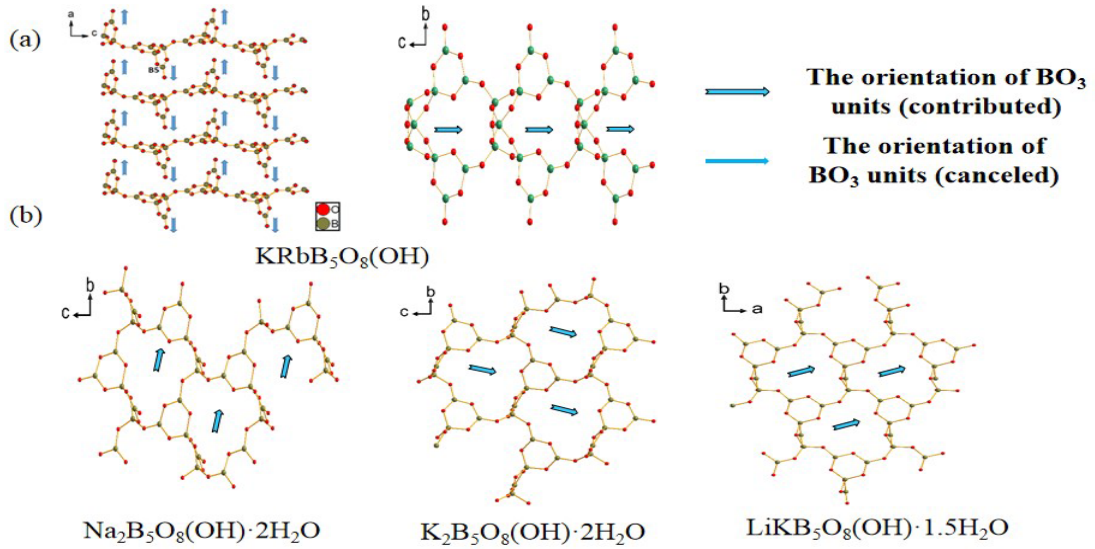

Figure S3. View of the layered stacked skeleton of $KRbB_5O_8(OH)$ down the *b*-, and *a*-axis; (b) View of the layered stacked skeleton of $Na_2B_5O_8(OH)\cdot 2H_2O$, $K_2B_5O_8(OH)\cdot 2H_2O$, $LiKB_5O_8(OH)\cdot 1.5H_2O$ down the *a*, *c*-axis.

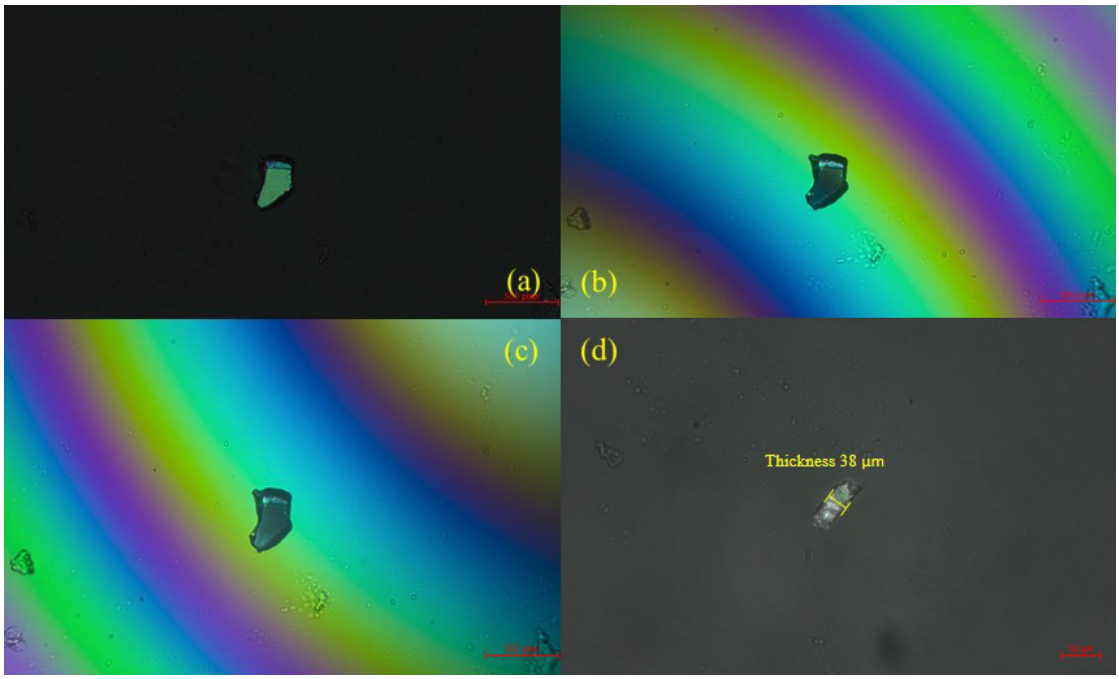

Figure S4. Birefringence measurement of $KRbB_5O_8(OH)$ using a polarizing microscope. (a) The original view of the crystal; (b, c) View of the crystal achieving extinction at the negative and positive rotation of the compensator, respectively; (d) Thickness of the crystal for measurement.

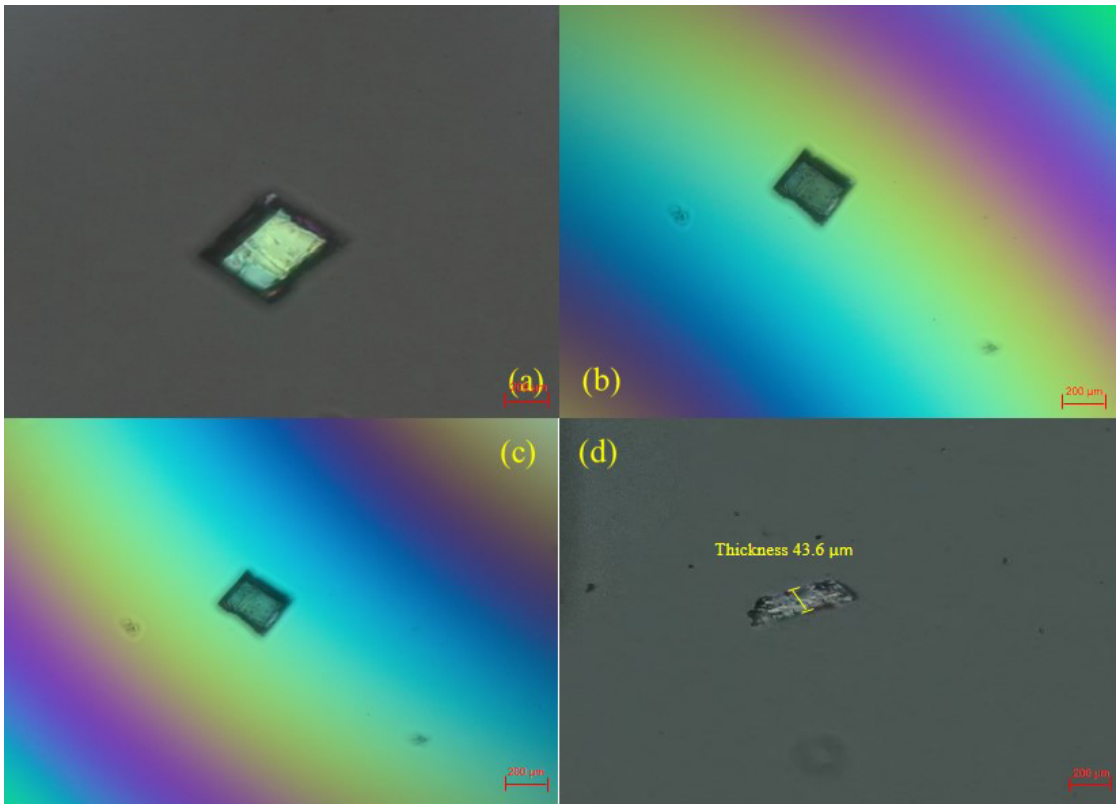

Figure S5. Birefringence measurement of $KRbB_6O_9(OH)_2$ using a polarizing microscope. (a) The original view of the crystal; (b, c) View of the crystal achieving extinction at the negative and positive rotation of the compensator, respectively; (d) Thickness of the crystal for measurement.

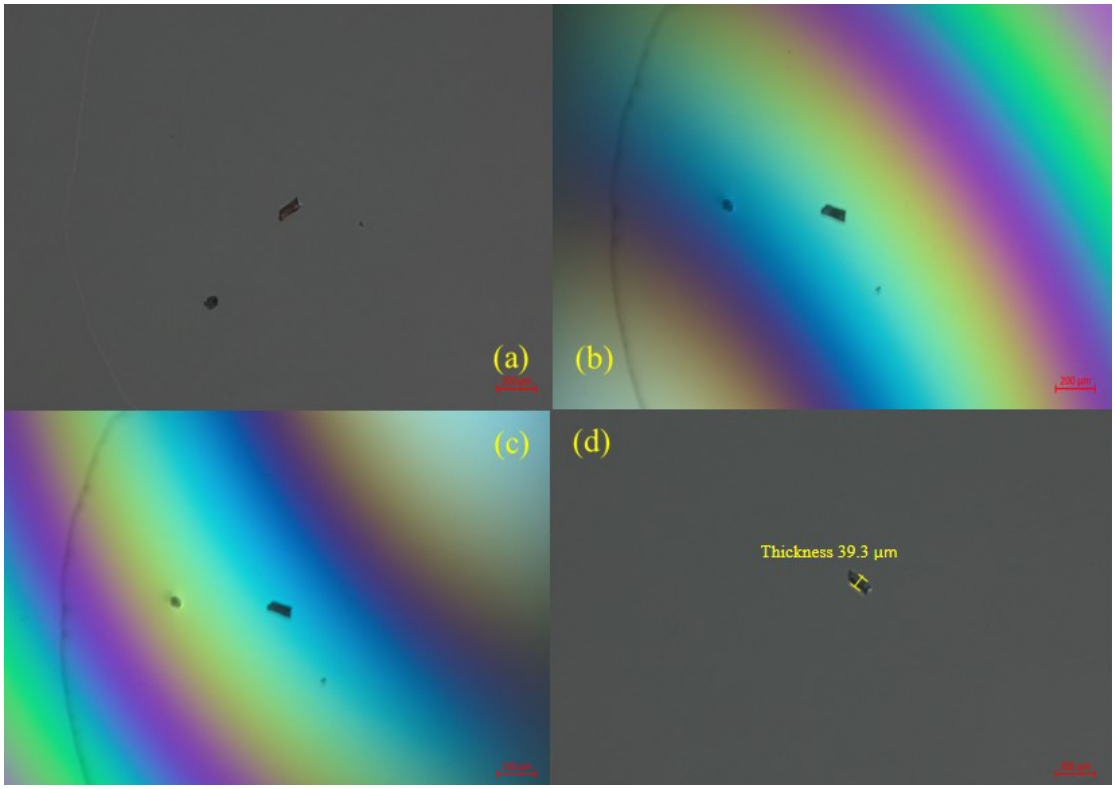

Figure S6. Birefringence measurement of $K_{3.3}Rb_{0.7}B_{10}O_{15}(OH)_4$ using a polarizing microscope. (a) The original view of the crystal; (b, c) View of the crystal achieving extinction at the negative and positive rotation of the compensator, respectively; (d) Thickness of the crystal for measurement.

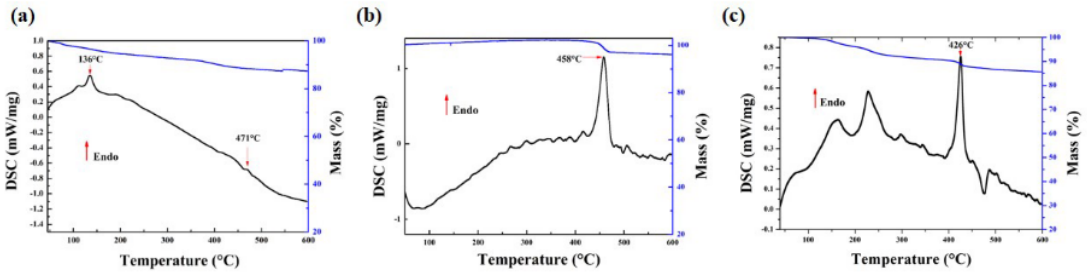

Figure S7. TG-DSC curves for (a) $KRbB_5O_8(OH)$; (b) $KRbB_6O_9(OH)_2$; (c) $K_{3.3}Rb_{0.7}B_{10}O_{15}(OH)_4$.

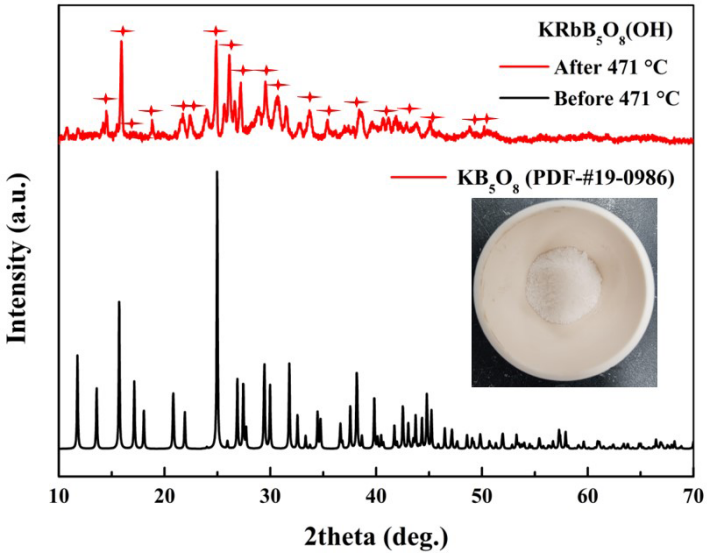

Figure S8. Experimental powder X-ray diffraction pattern of $KRbB_5O_8(OH)$ and photo of the after-melting experiment sample.

References

[1] B. H. Toby, R. B. Von Dreele, *J. Appl. Crystallogr.,* 2013, **46,** 544–549.

[2] SAINT, *Version 7.60A; Bruker Analytical X-ray Instruments,* Inc.: Madison, WI, **2008**.

[3] G. M. Sheldrick, SHELXTL, *Version 6.14; Bruker Analytical X-ray Instruments,* Inc.: Madison, WI, **2008**.

[4] A. L. Spek, *J. Appl. Cryst.,* 2003, **36,** 7–13.

[5] S. K. Kurtz, T. T. Perry, *J. Appl. Phys.,* 1968, **39,** 3798–3813.

[6] L. L. Cao, G. Peng, W. B. Liao, T. Yan, X. F. Long, N. Ye, *CrystEngComm.,* 2020, **22,** 1956–1961.

[7] S. J. Clark, M. D. Segall, C. J. Pickard, P. J. Hasnip, M. J. Probert, K. Refson, M. C. Payne, *Z. Kristallogr.,* 2005, **220,** 567–570.

[8] J. P. Perdew, K. Burke, M. Ernzerhof, *Phys. Rev. Lett.,* 1996, **77,** 3865–3868.

[9] J. S. Lin, A. Qteish, M. C. Payne, V. Heine, *Phys. Rev. B,* 1993, **47,** 8–15.

[10] A. M. Rappe, K. M. Rabe, E. Kaxiras, J. D. Joannopoulos, *Phys. Rev. B,* 1990, **41,** 2–15.

[11] C. S. Wang, M. Klein, *Phys. Rev. B,* 1981, **24,** 3417-3429.